Scientific Journal of Impact Factor (SJIF): 4.72

e-ISSN : 2348-4470
p-ISSN : 2348-6406

International Journal of Advance Engineering and Research Development

National Conference On Nanomaterials, (NCN-2017)

Volume 4, Special Issue 6, Dec.-2017 (UGC Approved)

Structural, morphological and dielectric studies of (0.5) $La_{0.8}Sr_{0.2}MnO_3$ + (0.5) $Ba_{0.5}K_{0.5}TiO_3$ composite

M. S. Malla and Dinesh Varshney[#]

Materials Science Laboratory, School of Physics, Vigyan Bhawan, Devi Ahilya University, Khandwa Road Campus, Indore 452001, India.

Abstract: *A composite of two homostructured materials i.e. perovskites (ABO_3) namely $Ba_{0.5}K_{0.5}TiO_3$ and $La_{0.8}Sr_{0.2}MnO_3$ has been prepared efficiently through ceramic synthesis route. The parent materials in ratio 1:1 were taken to make a composite. Analysis of the XRD data confirmed the single phased crystalline cubic structure with assigned space group Pm-3m. The single phaseness is found to occur due to higher sintering temperature. Using classical Scherer formula, the calculated particle size was found to be of the order of 36 nm. Retvield refinement of the data clears the structure and other essential parameters regarding structure. The surface morphology studies confirmed increase in average particle size and energy dispersive analysis of X-ray (EDAX) technique revealed the presence of all the constituents of the material under investigation. The dielectric studies were carried out and the sample was found to exhibit appreciable dielectric behaviour.*

Keywords*: Nanoparticles, Structure, Retvield refinement, morphology, dielectric properties.*

1. Introduction

Extensive research has been carried out on ABO_3-type manganites of the general formula $R_{1-x}A_xMnO_3$ (R = La, Nd, Pr, Y, etc. and A = Ca, Sr, Ba, Pb, etc.). Because of their extraordinary magnetic and electronic properties as well as their edge for the promising technological applications, these materials gained considerable attention [1, 2]. These compounds exhibit a high degree of chemical flexibility which together with a complex interplay between structures, electronic and magnetic properties leads to a very rich phase diagram involving various metallic, insulating and magnetic phases [3]. These properties are sensitive to the doping concentration x, which determine the Mn^{3+}/Mn^{4+} ratio to maintain charge neutrality, the average cationic radii and the ionic size mismatch between the various A-site ions.

$La_{0.8}Sr_{0.2}MnO_3$ (LSMO) belong to hole doped manganite and it is a potential candidate for technological applications because of its higher ferromagnetic transition temperature (T_C) around 370 K and a large magnetic moment at room temperature and high magnetoresistance (MR) value. The LSMO with the typical composition $La_{0.8}Sr_{0.2}MnO_3$ is broadly established as the cathode material for high temperature solid oxide fuel cells (SOFCs) [4]. The particle size and microstructure of electrode are significant for the electrode performance [5, 6]. Parent compound $LaMnO_3$, the antiferromagnetic insulator when doped with the divalent ions (A^{2+}), it is driven into a ferromagnetic metallic state as a result of conversion of Mn^{3+} to Mn^{4+} through double exchange (DE) mechanism [7].

Mason and Matthias suggested that Ti^{4+} ions are the influencing factor for ferroelectric nature of $BaTiO_3$ [8]. Barium titanate ($BaTiO_3$) is a ferroelectric oxide that undergoes a transition from a ferroelectric tetragonal phase to a paraelectric cubic phase upon heating above 130 °C. In cubic perovskite $BaTiO_3$, titanium atoms are octahedrally coordinated by six oxygen atoms. Ferroelectricity in tetragonal $BaTiO_3$ arises due to an average relative displacement along the c-axis of titanium from its centrosymmetric position in the unit cell and consequently the creation of a permanent electric dipole. The elongation of the unit cell along the c-axis and consequently the deviation of the c/a ratio from unity are used as an indication of the presence of the ferroelectric phase [9, 10]. $BaTiO_3$ is particularly challenging since it exhibits three solid-solid phase transitions. $BaTiO_3$ is the most important perovskite (ABO_3) oxide with excellent dielectric and ferroelectric properties. For improvement in the performance and miniaturization of electronic devices using $BaTiO_3$ based materials, it is important to ensure the high dielectric constant, low dielectric loss, high remnant polarization and high dielectric strength and hence is the subject of modification. A-site substitution often comes from alkaline-earth (Sr^{2+} or Mg^{2+}), alkali metals (Na^+, K^+) and rare-earth ions (La^{3+} etc.) whose cation size effects suppress Ti off-centering thus lower the Curie temperature. The high dielectric permittivity combined with low dissipation factor makes it one of the promising candidates for dynamic random access memory, decoupling capacitors and dielectric field tunable elements for high frequency device applications [9].

The aim of the project is to seek the magnetoelectric effect that is why we have chosen well known doped ferromagnetic ($La_{0.8}Sr_{0.2}MnO_3$) and ferroelectric ($Ba_{0.5}K_{0.5}TiO_3$) materials. Howsoever, in the present piece of work, we are presenting an attempt to explore the collective effects on the structure, morphology and dielectric properties of the composite.

2. Experimental Details

(0.5) $La_{0.8}Sr_{0.2}MnO_3$ (LSMO) + (0.5) $Ba_{0.5}K_{0.5}TiO_3$ (BKT) sample was prepared by the conventional ceramic fabrication technique of solid-state reaction. The starting analytic grade materials were La_2O_3, MnO_2, $SrCO_3$, $BaCO_3$, K_2CO_3 and TiO_2. Lanthanum and manganese oxides together with strontium carbonate were mixed in stoichiometric amounts to prepare manganite $La_{0.8}Sr_{0.2}MnO_3$ and barium and potassium carbonate along with titanium oxide were mixed in stoichiometric proportions to prepare $Ba_{0.5}K_{0.5}TiO_3$. These mixtures were ground and calcined in air at 1250 °C and 1050 °C for 24 h with intermediate grinding of about 15 h. The fine powders obtained were pressed into pellet form of the diameter of 10 mm under a pressure of 8 tons created by hydraulic press and finally sintered in air at 1300 °C and 1100 °C for 24 h each. The equal amount of the above powders was mixed in an agate-mortar for more than three hours to ensure homogeneous dispersion of the phases into one another. Before making pellet, the mixture was added with binder [poly-vinyl alcohol (PVA) as matrix] and ground again to ensure the proper dispersion of the embedding material in the matrix. The pellet as above was prepared and sintered at 1300 °C for 10 hours.

X-ray powder diffraction technique at room temperature is used to identify the crystal structure, type of phase and crystallite size of $La_{0.8}Sr_{0.2}MnO_3$ nanopowder by means Bruker D8-Advance X-ray diffractometer with Cu$K\alpha_1$ (1.5406 Å) radiation. The data was collected with a step size of 0.02° over the angular range 2θ (10° < 2θ < 80°) generating X-ray by 40 kV and 40 mA power settings. Rietveld refinement was done on the XRD data using FullProf refinement software.

Scanning electron micrographs and energy dispersive spectrum analysis of X-ray diffraction was obtained using SEM instrument model JEOL JSM-5600 with a resolution of 3.5 nm, magnification power of x 18-300000 kV (in 136 steps), acceleration voltage of 0.5-30 kV (53 steps) and energy dispersive spectrometer, model INCA Oxford. Dielectric measurements were performed as a function of frequency in the range of 20Hz–1MHz on Novocontrol alpha-A high performance frequency analyzer at room temperature.

3. Results And Discussion

3.1. Structural Analysis

The prepared sample (0.5) $La_{0.8}Sr_{0.2}MnO_3$ + (0.5) $Ba_{0.5}K_{0.5}TiO_3$ powder has been structurally characterized by X-ray powder diffraction (XRD). XRD was used to determine the phase structure and purity of the as-synthesized samples. Room temperature XRD pattern of (0.5) $La_{0.8}Sr_{0.2}MnO_3$ + (0.5) $Ba_{0.5}K_{0.5}TiO_3$ sample is shown in Figure 1. Analysis of the XRD pattern revealed the cubic structure of the sample with the assigned space group *Pm*-3*m*. Though attempt was the preparation of the composite of the perovskite (ABO_3) types of ferroelectric BKT and ferromagnetic LSMO but due to heat treatment at higher temperature i.e. 1300 °C, there has occurred a new phase. This is because the ionic radii of the A-site La, Ba, K and B-site Ti, Mn of ABO_3 are comparable and their inter-diffusion has been facilitated by high temperature treatment resulting in the formation of a single phased material. The purity and single phase nature is also evident due to absence of any extra peak within the experimental limit. The broadness of characteristic XRD peaks is due the nano size effect and the sharpness of the same peak is attributed to the high crystallinity of samples.

The average particle size (d) of the samples is calculated by classical Debye-Scherrer's formula [11]:

$d = 0.9\lambda/\beta\cos\theta$

where, λ is the wavelength of Cu$K\alpha_1$ radiation used and β is the full width half maximum (FWHM) of the highest intense peak of diffracting angle 2θ. The average calculated particle size was about 36 *nm*.

The XRD pattern was analyzed using Rietveld method and the refinement confirmation for crystal structure was carried out using the FULLPROF program [12].

Figure 2 shows Rietveld refinement of room temperature XRD pattern of (0.5) $La_{0.8}Sr_{0.2}MnO_3$ + (0.5) $Ba_{0.5}K_{0.5}TiO_3$. The cubic structure of the sample has been confirmed along with the space group of *Pm*-3*m*. All the structural parameters obtained by Retvield refinement are given in the Table 1.

3.2. Microstructural Analysis

Scanning electron microscopy was employed to investigate the morphology of the samples. Figure 3 shows the micrograph of (0.5) $La_{0.8}Sr_{0.2}MnO_3$+ (0.5) $Ba_{0.5}K_{0.5}TiO_3$ nanocrystals. The nano particles obtained in (0.5) $La_{0.8}Sr_{0.2}MnO_3$ +(0.5) $Ba_{0.5}K_{0.5}TiO_3$ are nearly spherical in shape. All compositions have grains with sharp boundaries indicating that grains are fully developed, well packed, crack free with clear grain boundaries. The SEM micrographs illustrates the morphology is well ordered, having aggregation and better particle size distribution. The homogeneity of the samples is the indication of single phase nature of the sample. From the SEM micrograph it is clear that as synthesized samples display the piling by virtue of diffusion process of smaller nanoparticles. From SEM image, the average grain size of sample under investigation is found of micrometer range due to sintering at higher temperature along with obivious grown boundaries.

3.3. Energy-dispersive analysis of X-ray (EDAX) spectra

The chemical compositional analysis of (0.5) $La_{0.8}Sr_{0.2}MnO_3$ + (0.5) $Ba_{0.5}K_{0.5}TiO_3$ nanoparticles have been carried out using EDAX. The EDAX spectra of (0.5) $La_{0.8}Sr_{0.2}MnO_3$ + (0.5) $Ba_{0.5}K_{0.5}TiO_3$ is shown in Figure 4. The EDAX spectra reveals the presence of lanthanum, manganese, potassium, titanium, strontium, barium and oxygen suggesting that the sample is indeed made up of only these metal ions and there is no loss of the constituents of the sample. Meanwhile, the intensity of strontium and potassium related peaks are smaller than the peaks of other constituents of the sample which is due their lower concentration in the sample.

3.4. Dielectric measurement

Studies have been carried out on (0.5) $La_{0.8}Sr_{0.2}MnO_3$+ (0.5) $Ba_{0.5}K_{0.5}TiO_3$ sample to investigate the combined effect on dielectric constant when a ferromagnetic metallic phase is introduced in ferroelectric phase. The real part (ε') of dielectric constant is the measure of the amount of energy stored in a dielectric due to the applied field and is calculated by using formula $\varepsilon = Ct/A\varepsilon_0$ where ε_0 is the permittivity of free space, '*t*' is the thickness of pellet, 'A' is the cross sectional area and '*C*' is the capacitance of pellet. Figure 5 shows the variation of ε' with frequency for (0.5) $La_{0.8}Sr_{0.2}MnO_3$ + (0.5) $Ba_{0.5}K_{0.5}TiO_3$ at room temperature. It is obvious from the Figure 5 that for the prepared sample, dielectric constant (ε') decreases with increase in frequency (*f*) and becomes constant at higher values of frequency. This variation of ε' with *f* reveals the dispersion due to Maxwell-Wagner [13] type interfacial polarization and is in agreement with Koop's phenomenological theory [14]. The high values of dielectric constant at low frequencies may be due to the interfacial dislocations, oxygen vacancies, charged defects, grain boundaries effect and interfacial/space charge polarization due to heterogeneous dielectric structure.

The variation of loss tangent (tan δ) with frequency at room temperature is shown in Figure 6. At high frequencies, the dielectric loss decreases due to the suppression of domain wall motion. The dielectric loss is found to be maximum at lower frequencies. This results when the hopping frequency of electrons between different ionic sites becomes nearly equal to the frequency of the applied field. The dielectric loss arises if the polarization lags behind the applied alternating field which is introduced by the presence of impurities and structural inhomogeneities. The value of dielectric loss tangent is high at low frequency and progressively reduces and attains a constant value at higher frequency region [15]. In the present study, the dielectric loss attains a maximum value at a particular frequency. This characteristic is attributed to the resonance between the applied electric field and the polaron hopping frequency [16]. The intriguing values of dielectric constant and dielectric loss at low and high frequency are given in the Table 2.

4. Conclusion

We have successfully prepared a single phased and pure material using ceramic route i.e. solid state reaction method while trying for composite (0.5) $La_{0.8}Sr_{0.2}MnO_3$ + (0.5) $Ba_{0.5}K_{0.5}TiO_3$. This is because of high temperature treatment and comparable ionic radii of the constituent elements of parent perovskite compounds corresponding to their A- and B- sites. XRD analysis confirmed the cubic structure of the new born compound with space group *Pm*-3*m*. The Retveld refinement further confirms the structure and the space group and the various structural parameters obtained are highly appreciable. Microstructural studies confirmed the growth of average particle size due to sintering at higher temperature. EDAX analysis confirmed the presence of all the constituent elements of the sample and the presence of their appreciable concentration. Dielectric measurements reveal that the sample exhibits an admirable dielectric constant which reduces with the increase in the frequency. The same behaviour is observed for dielectric loss where at low frequency, the loss is high which decreases with increase in the frequency. The results seem to be interesting and needs further attention.

Acknowledgements

UGC-DAE-CSR, as an institute is acknowledged for providing characterization facilities. Authors are thankful to Dr. M. Gupta, Dr. A. M. Awasthi, Dr. D. M. Phase for their guidance and useful discussions and engineers namely Lyantha, Suresh Bharadwaj, V. K. Ahire for providing data timely.

References

[1] X.F. Zhou, Y. Zhao, X. Cao, Y.F. Xue, D. P. Xu, L. Jiang, W.H. Su, *Mater. Lett*. 62, 47 (**2008**)
[2] L. Millar, H. Taherparvar, N. Filkin, P. Slater, J. Yeomans, *Solid State Ion*. 179, 73 (**2008**).
[3] P. K. Siwatch, H.K. Siugh, O.N. Srivastava: *J. Phys. Condens. Matter.*, 20, 273201 (**2008**)
[4] A. Chainani, M. Mathew, D. D. Sarma, *Phys. Rev. B*, 47**,** 15397(**1993**).
[5] Rodriguez - Martinez, L. M., Attfield, J. P. *Phys. Rev. B***.,** 54, 15622 (**1996**).
[6] P. V. Vanitha, P.N.S. Santosh, R. S. Singh, C.N.R. Rao, J.P. Attfield: *Phys. Rev. B*, 59, 13539 (**1999**).
[7] C. Zener, *Phys. Rev*., 82, 403 (**1951**).
[8] W. P. Mason, and B. T. Matthias, *Phys. Rev*., 74**,** 1622 (**1948**).
[9] M. B. Smith, K. Page, T. Siegrist, P. L. Redmond, E. C. Walter, R. Seshadri, L. E. Brus, and M. L. Steigerwald, *J. Am. Chem. Soc.*, 130, 6955 (**2008**).
[10] B. A. Strukov, A. P. Levanyuk, *Springer-Verlag, Berlin*, **1998**.
[11] L. Broussous, C. V. Santilli, S. H. Pulcinelli, A. F. Craievich, *J. Phys. Chem.*, B 106, 2885 (**2002).**
[12] J. Rodriguez - Carvajal, *Physica B*, 192**,** 55 (**1993**).
[13] J. C. Maxwell, Electricity and Magnetism (Oxford University Press, New York), **1,** 828 (**1973**).
[14] C. G. Koops, *Phys. Rev*., 83**,** 121 (**1951**).
[15] D. Ravinder, K. Vijayakumar, *Bull. Mater. Sci*., 24**,** 505 (**2001**).
[16] M. Saleem, D. Varshney, *Journal of Alloys and Compounds*, 708, 397 (**2017**) and D. Varshney, K. Verma, *Mater. Chem. Phys.*, 140**,** 412 (**2013**).

Figure Captions

Figure 1: Shows the X-Ray diffraction pattern of the (0.5) $La_{0.8}Sr_{0.2}MnO_3$ + (0.5) $Ba_{0.5}K_{0.5}TiO_3$ composite.

Figure 2: depicts the refinement of the XRD data of the (0.5) $La_{0.8}Sr_{0.2}MnO_3$ + (0.5) $Ba_{0.5}K_{0.5}TiO_3$ composite.

Figure 3: SEM Micrograph of the (0.5) $La_{0.8}Sr_{0.2}MnO_3$ + (0.5) $Ba_{0.5}K_{0.5}TiO_3$composite.

Figure 4: EDAX spectra of the (0.5) $La_{0.8}Sr_{0.2}MnO_3$ + (0.5) $Ba_{0.5}K_{0.5}TiO_3$composite.

Figure 5: Dielectric constant of the (0.5) $La_{0.8}Sr_{0.2}MnO_3$ + (0.5) $Ba_{0.5}K_{0.5}TiO_3$ sample.

Figure 6: Dielectric loss of the (0.5) $La_{0.8}Sr_{0.2}MnO_3$ + (0.5) $Ba_{0.5}K_{0.5}TiO_3$ sample.

Structural, morphological and dielectric studies of
(0.5) $La_{0.8}Sr_{0.2}MnO_3$ + (0.5) $Ba_{0.5}K_{0.5}TiO_3$ composite

M. S. Malla and Dinesh Varshney

Figure 1:

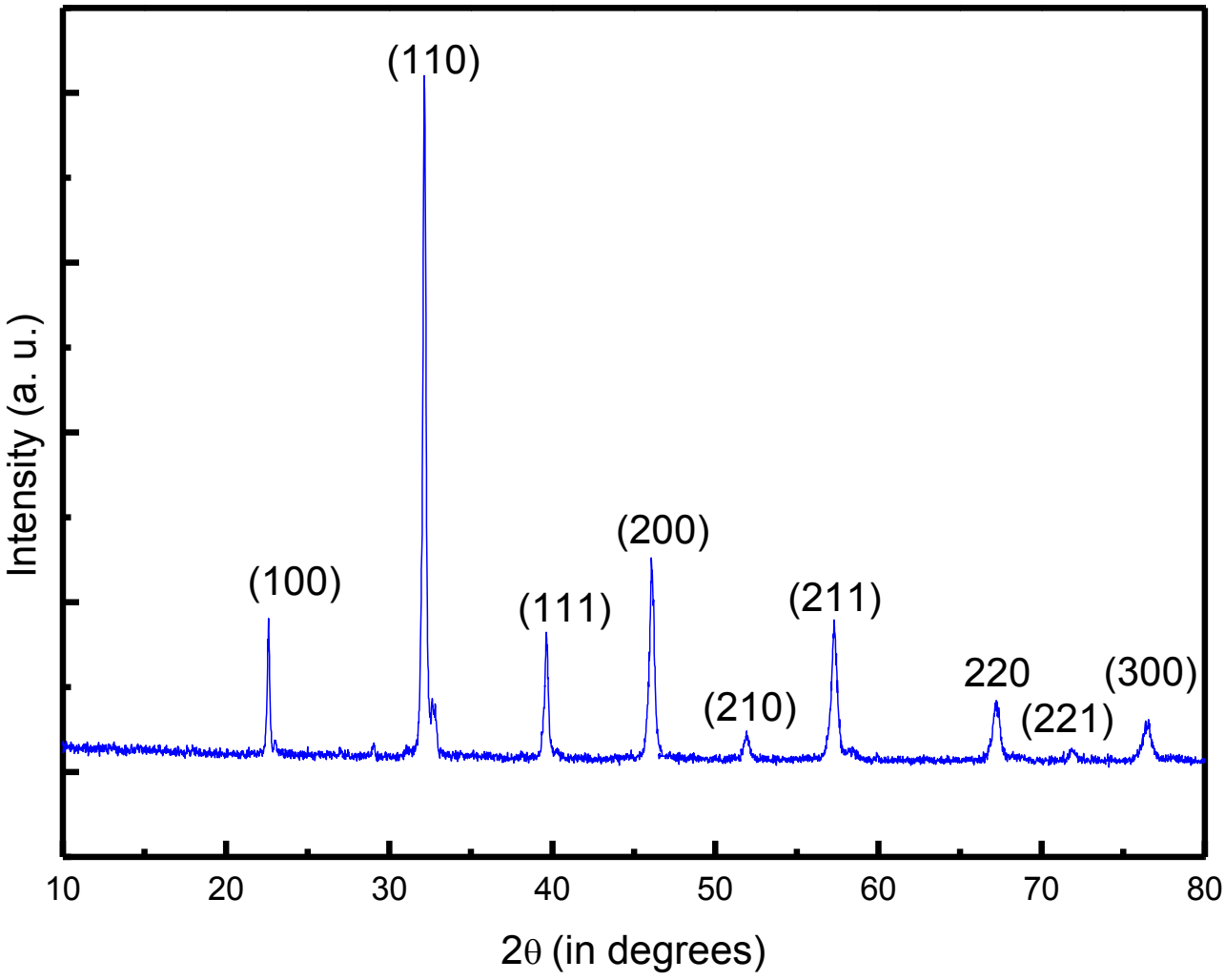

Structural, morphological and dielectric studies of
(0.5) $La_{0.8}Sr_{0.2}MnO_3$ + (0.5) $Ba_{0.5}K_{0.5}TiO_3$ composite

M. S. Malla and Dinesh Varshney

Figure 2 (colour):

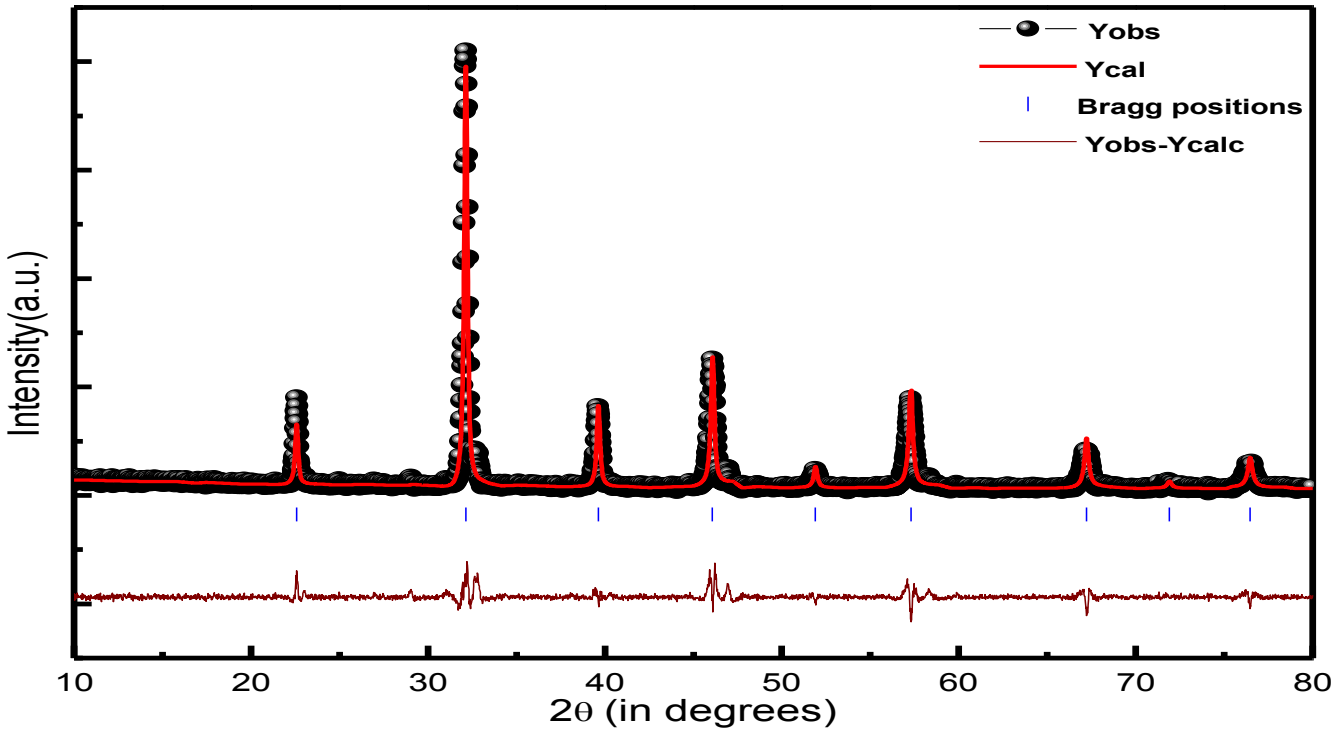

Structural, morphological and dielectric studies of
(0.5) $La_{0.8}Sr_{0.2}MnO_3$ + (0.5) $Ba_{0.5}K_{0.5}TiO_3$ composite

M. S. Malla and Dinesh Varshney

Figure 3:

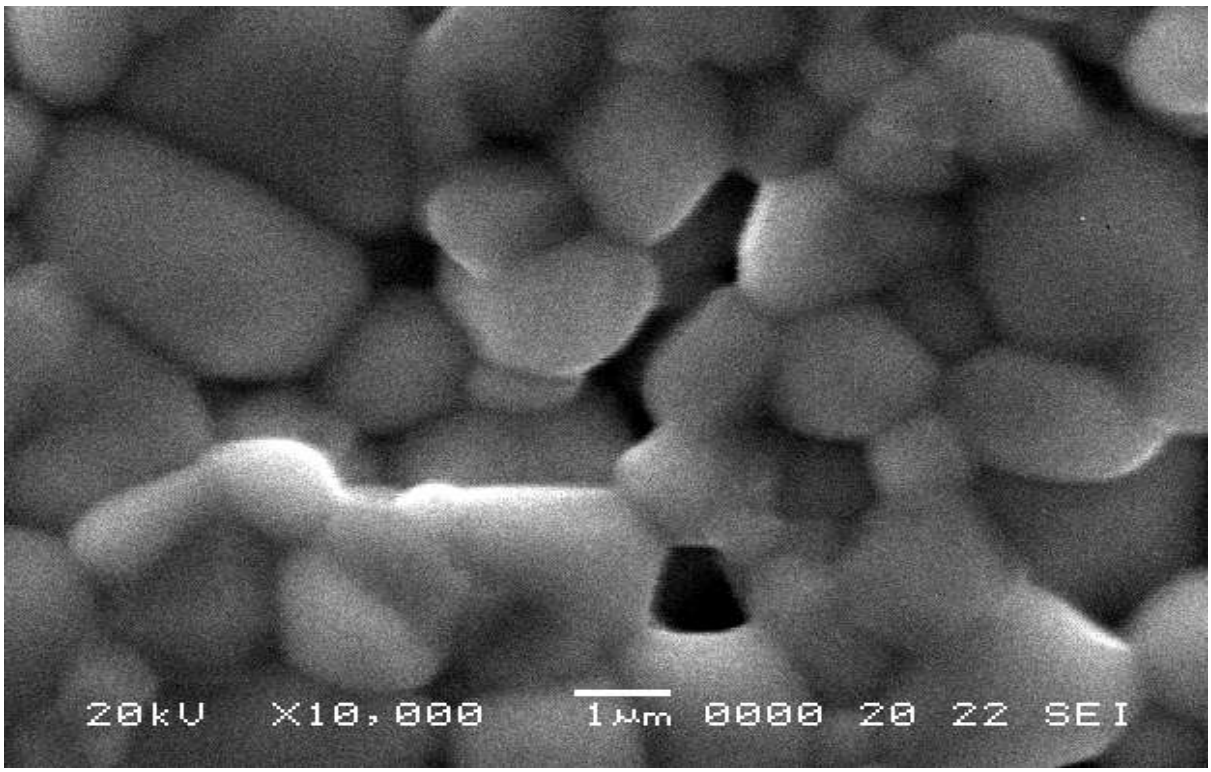

Structural, morphological and dielectric studies of (0.5) $La_{0.8}Sr_{0.2}MnO_3$ + (0.5) $Ba_{0.5}K_{0.5}TiO_3$ composite

M. S. Malla and Dinesh Varshney

Figure 4:

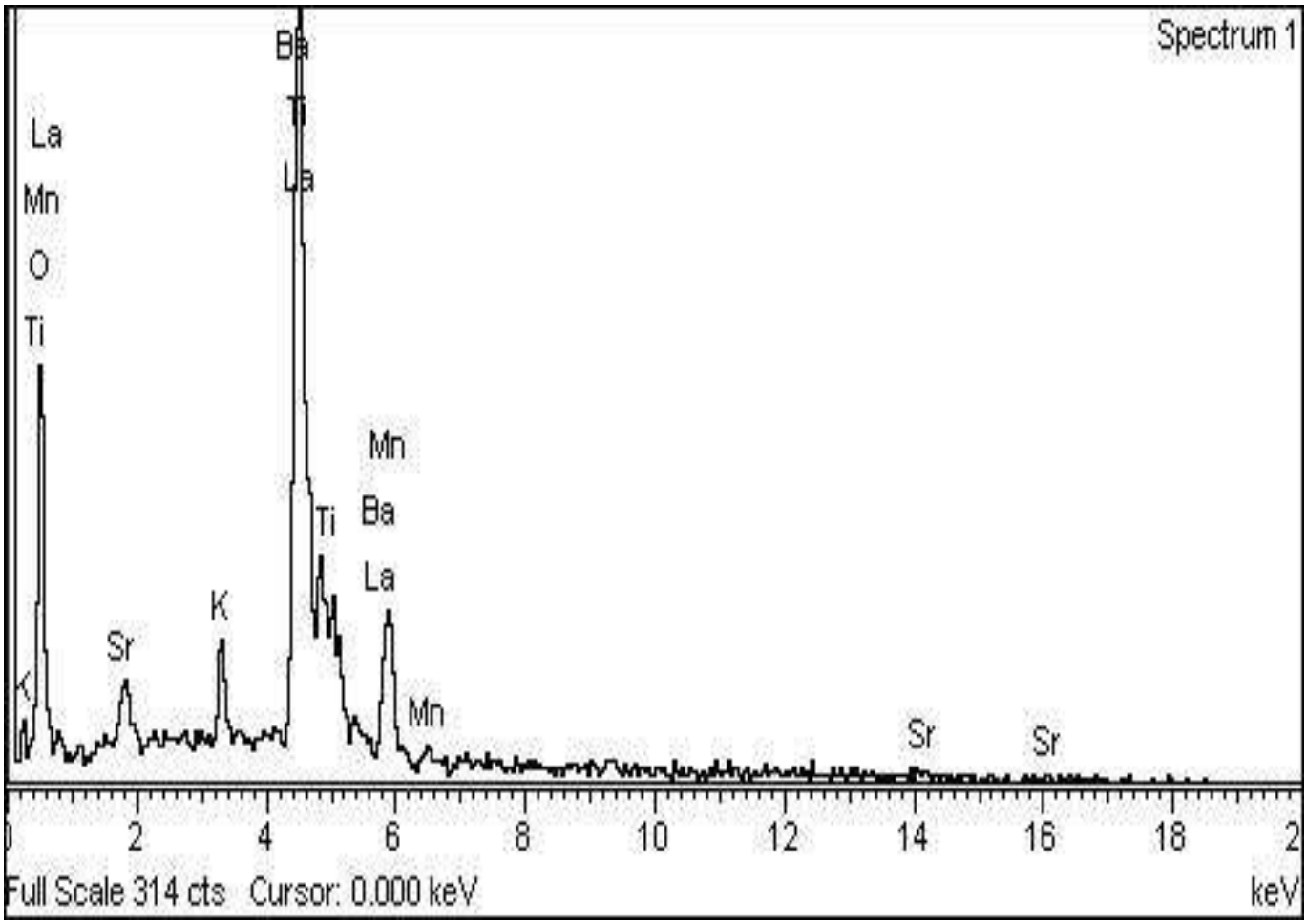

Structural, morphological and dielectric studies of (0.5) $La_{0.8}Sr_{0.2}MnO_3$ + (0.5) $Ba_{0.5}K_{0.5}TiO_3$ composite

M. S. Malla and Dinesh Varshney

Figure 5 (colour):

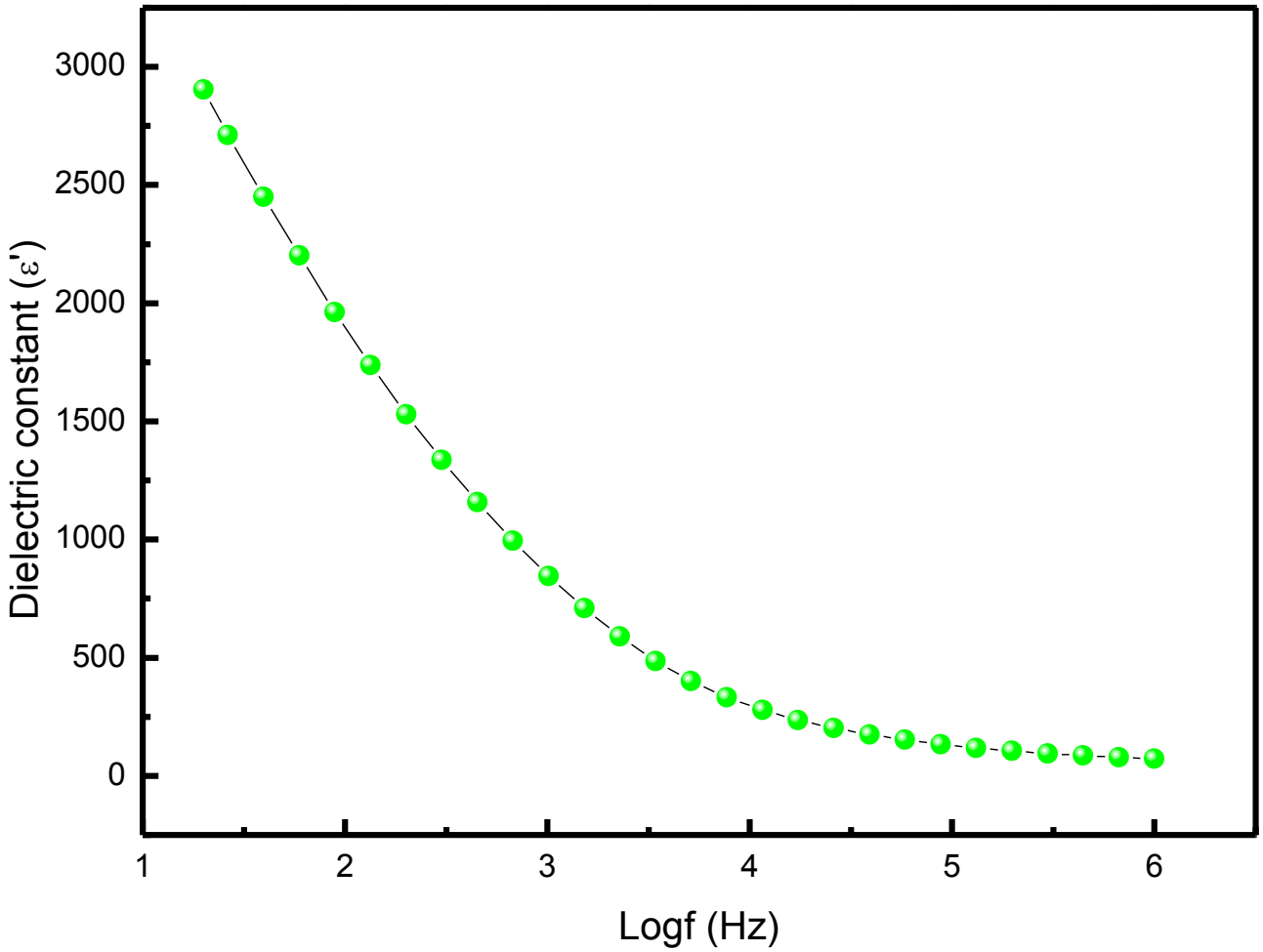

Structural, morphological and dielectric studies of
(0.5) $La_{0.8}Sr_{0.2}MnO_3$ + (0.5) $Ba_{0.5}K_{0.5}TiO_3$ composite

M. S. Malla and Dinesh Varshney

Figure 6(colour):

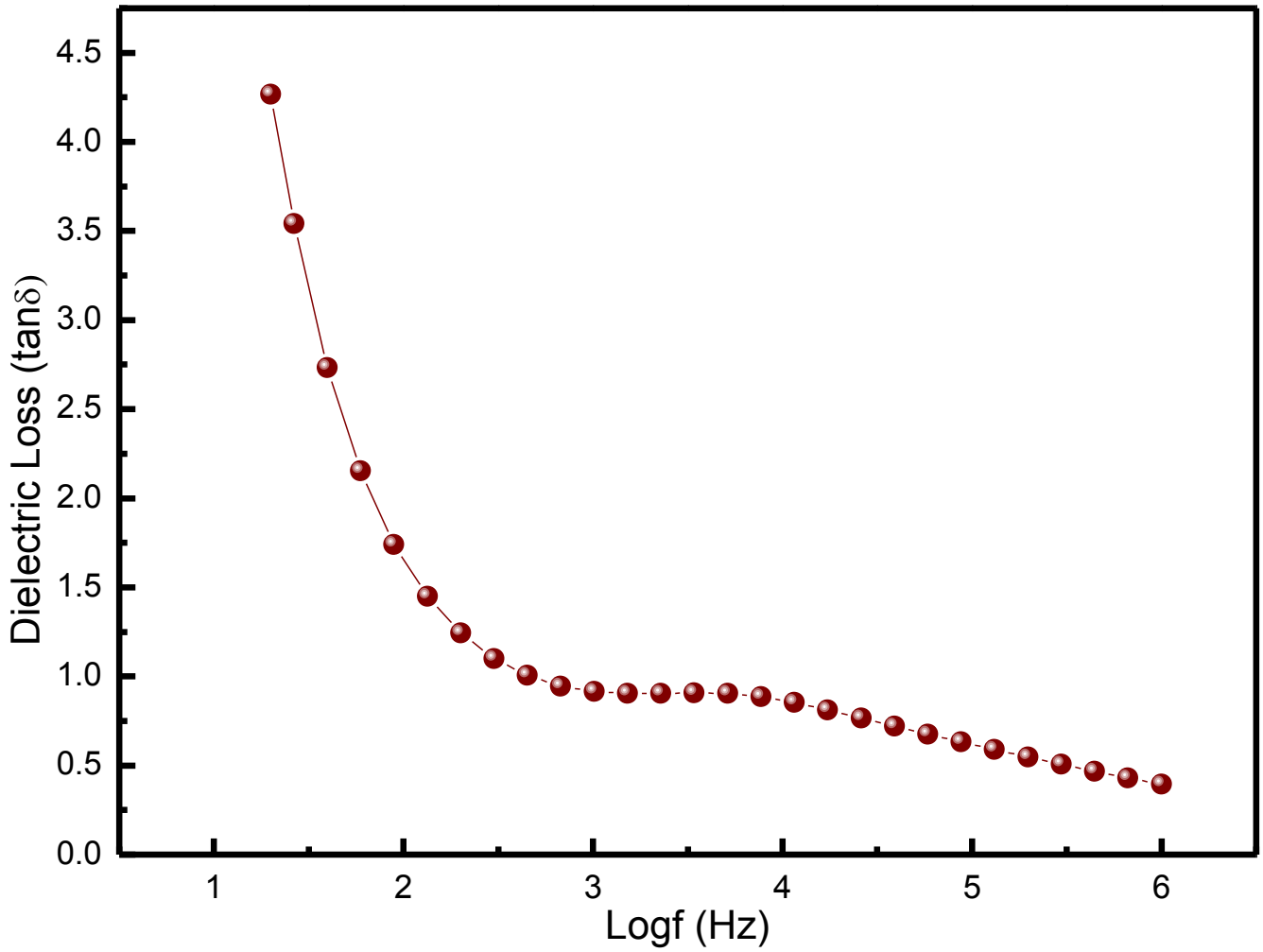

Structural, morphological and dielectric studies of
(0.5) $La_{0.8}Sr_{0.2}MnO_3$ + (0.5) $Ba_{0.5}K_{0.5}TiO_3$ composite
M. S. Malla and Dinesh Varshney
Table 1:

Table 1: Details of Rietveld refined XRD pattern of the (0.5) $La_{0.8}Sr_{0.2}MnO_3$ + (0.5) $Ba_{0.5}K_{0.5}TiO_3$

Parameters	Values obtained
Space group	*Pm-3m*
a (Å)	3.936(3)
V (Å^3)	60.998
Density (g / cm^3)	12.430
La / Sr/ Ba / K (*x*, *y*, *z*)	(0.5, 0.5, 0.5)
Mn / Ti (*x*, *y*, *z*)	(0.0, 0.0, 0.0)
O (*x*, *y*, *z*)	(0.0, 0.0, 0.0)
Bond distance	
La / Sr / Ba / K – O	2.78 (2) Å
Mn / Ti-O	1.968 (3) Å
R_F	6.38
R_{Braqg}	10.40
R_p	32.4
R_{wp}	30.8
R_{exp}	20.7
χ^2	2.216
GOF	1.5

Table 2:

Table 2: Dielectric parameters of the (0.5) $La_{0.8}Sr_{0.2}MnO_3$ +(0.5) $Ba_{0.5}K_{0.5}TiO_3$

At	Dielectric constant	Dielectric loss
20 Hz	2903.7	4.2688
10^6Hz	71.7	0.39528

s

